JOURNAL OF CATALYSIS **131,** 319–325 (1991)

Shape Selectivity in Porous Catalysts

C. McGREAVY,[1,*] J. S. ANDRADE, JR.,[†] AND K. RAJAGOPAL[†]

**Department of Chemical Engineering, University of Leeds, Leeds, England LS2 9JT; and †Programa de Engenharia Química, COPPE, Universidade Federal do Rio de Janeiro, CP 68502, Rio de Janeiro, RJ, Brasil*

Received June 15, 1990; revised May 13, 1991

The shape selectivity of porous catalysts is examined with reference to the detailed structural arrangement of pore sizes. As a conceptualization of the pellet structure, an array of cylindrical capillaries comprising pores of two sizes with a distribution function specified in terms of the smaller pore is used. A generic case study based on a complex reaction scheme is considered. It involves a set of parallel and reversible first-order reactions which take place in the larger pores, with one of the products being diffusionally limited in the smaller capillaries because of sterically hindered transport. Simulation of the detailed interactions between the kinetics and the diffusion clearly indicates the way in which the structure can have a dramatic influence on the selectivity of the unhindered product. Specifically, it reveals how the pore size distribution can influence the effective tortuosity of the diffusion path, and the way in which bottleneck cavities can be used to improve selectivity.

1. INTRODUCTION

Product selectivity is a distinctive feature of some modified zeolite catalysts operated under diffusion-limited conditions. For example, *para*-xylene selectivity can be enhanced by impregnation of the catalyst with compounds of phosphorus or boron (*1–3*). This is generally explained in terms of a shape selectivity effect associated with the diffusional mechanism at the molecular level which influences the reaction sequence in the intraparticle pore volume (*4, 5*). Figure 1 shows a schematic description of selective production of *para*-xylene in a confined pore from methanol alkylation of toluene. Only the *para* isomer can escape so that the reaction progressively favours the overall production of this species.

In a catalyst pellet the pore volume is generally made up of a complex pattern of pores of various sizes. In the case of zeolites, for example, partial cation exchange (*6*), coke deposition, and impregnation with phosphorus and boron compounds (*1*) can dramatically change the regular pore structure of the crystal. Characterizing this in a way which captures the overall pattern of behaviour requires a conceptual description which represents all the significant elements in an idealized framework. Network models have been widely employed in this way to describe diffusion and reaction in porous media (*7–10*). Recent work by Mann and Sharrat (*11*) was directed to the problem of an isomerization reaction in a stochastic pore network but did not allow for differences in diffusion coefficients in the isomers. Comparison with a classical pore volume model made up of a parallel bundle of capillaries shows that the traditional approach cannot provide a realistic interpretation of the selectivity mechanism in heterogeneous catalysis.

Shape selectivity can be expected to provide a very useful enhancement with respect to specific products but it depends on hindered diffusion coefficients of the species arising from steric effects on the

[1] To whom correspondence should be addressed.

0021-9517/91 $3.00

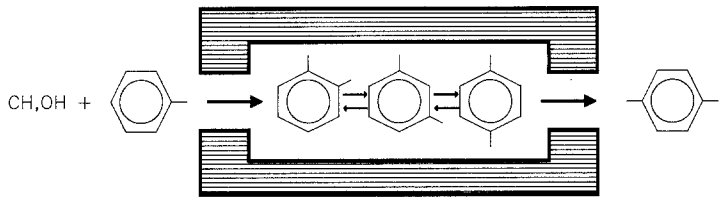

FIG. 1. Schematic representation of the *para*-xylene shape selectivity reaction from the methanol alkylation of toluene in a confined pore.

transport process. This study is directed towards developing a methodology which allows the structural effect of the pore volume size distribution on the shape selectivity and hence reactor *product selectivity* to be explored.

2. NOMENCLATURE

$\mathbb{C}_m$ – mobile phase concentration vector [ML^{-3}]
$\mathbb{C}$ – capillary concentration vector [ML^{-3}]
$\mathbb{D}$ – diffusivity matrix [L^2T^{-1}]
$\mathbb{K}$ – reaction rate constant matrix [T^{-1}]
L – reactor length [L]
l_p – particle length [L]
l – capillary length [L]
N – network dimension
$\mathbb{N}$ – molar flux vector [MT^{-1}]
pl – frequency distribution of pores
R – pore radius [L]
$\mathcal{S}_B$ – selectivity of product B
$\langle v \rangle$ – interstitial velocity of the mobile phase [LT^{-1}]
X' – axial coordinate in the reactor [L]
X – dimensionless axial coordinate in the reactor
x – axial coordinate in the capillary [L]

Subscripts

i – related to node i
j – related to node j
R – related to the reagent
A – related to the product A
B – related to the product B

Greek Symbols

α – radius factor
ε_C – column porosity
ε_P – particle porosity
ϕ – Thiele modulus
τ – reactor retention time [T]
χ_R – reagent conversion

3. PHYSICOCHEMICAL SYSTEM

As a representative problem, consider a plug flow reactor in which the following first-order isothermal reaction sequence occurs:

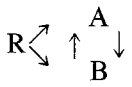

The catalyst pore structure at any point in the bed is assumed to be represented by a two-dimensional square network of cylindrical pores of fixed length (l) connected to sites or nodes of negligible volume (Fig. 2). The pellet is assumed to be made up of pores having a radius of either R_1 or R_2 according to a fixed frequency distribution (pl) of the smaller radius (R_1). Also, the pore radii are related by

$$R_1 = \alpha R_2 \tag{1}$$

where α is termed a pore radius factor. The spatial arrangement of both types of capillaries in the newtork can then be generated using a routine for random permutation of vectors.

For the class of problems under consideration, the smaller pores can be assumed to be formed as a consequence of partial coking or fouling. Alternatively, in the case of zeolites, they can be regarded as equivalent to the connections between the cages where the catalyst is located, as occurs, for example, in the channel intersections of ZSM-5

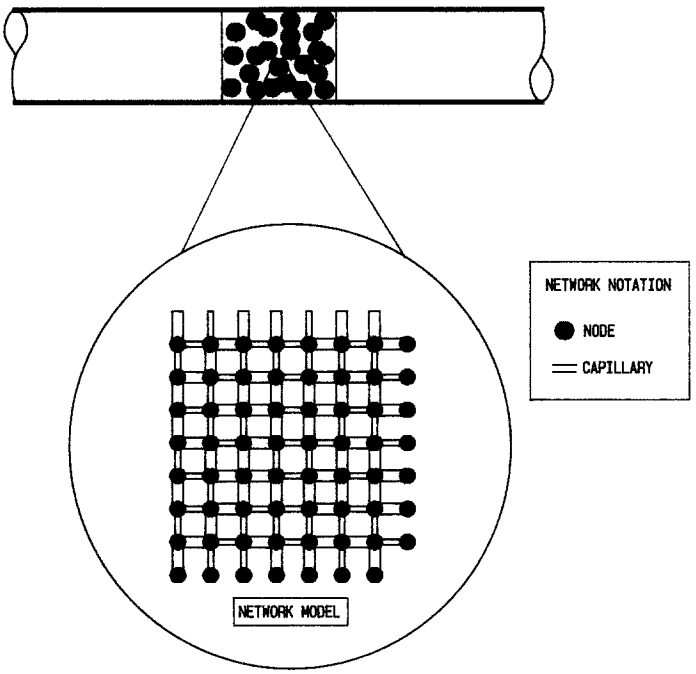

FIG. 2. Schematic representation of the plug flow reactor with the network description of the catalyst pore volume employed in the simultations.

zeolites (*12*). This means that reaction would only be expected in the larger pores, but this in no way is a limitation of the model used. There is no difficulty in allowing for reaction in both kinds of pore, but this particular situation reveals interesting characteristics to illustrate the approach.

4. MATHEMATICAL FORMULATION

Between two nodes (i) and (j) of the network, the concentration vector ($\mathbb{C}(x, t)$) representing the species is described by the mass balance

$$\mathbb{D}\nabla^2\mathbb{C} = \mathbb{K}\mathbb{C}; \quad \mathbb{K} = \mathbb{K}(R_{(i,j)}) \text{ and } \mathbb{D} = \mathbb{D}(R_{(i,j)}), \quad (2)$$

where $\mathbb{D}$ is the diffusivity matrix assumed to be diagonal and $\mathbb{K}$ is the rate constant matrix for the reaction sequence. For the three-component reaction–diffusion system,

$$\mathbb{D} = \mathbb{D}(R_{(i,j)}) = D_0 \begin{bmatrix} D_R & 0 & 0 \\ 0 & D_A & 0 \\ 0 & 0 & D_B \end{bmatrix} \quad \text{and}$$

$$\mathbb{K}(R_1) = \mathbb{O}$$

$$\mathbb{K}(R_2) = K_0 \begin{bmatrix} K_{RA} + K_{RB} & -K_{AR} & -K_{BR} \\ -K_{RA} & K_{AR} + K_{AB} & -K_{BA} \\ -K_{RB} & -K_{AB} & K_{BR} + K_{BA} \end{bmatrix}.$$

From Eq. (2), using the inverse of the diffusivity matrix $\mathbb{D}^{-1}$,

$$\nabla^2\mathbb{C} = \mathbb{D}^{-1}\mathbb{K}\mathbb{C}. \quad (3)$$

Introducing the boundary conditions as the unknown internal nodal concentration vectors,

$$\mathbb{C}(0) = \mathbb{C}_{(i)} \quad \text{and} \quad (4)$$

$$\mathbb{C}(l) = \mathbb{C}_{(j)}.$$

Diagonalizing $\mathbb{D}^{-1}\mathbb{K}$ we define

$$\mathbb{D}^{-1}\mathbb{K} = \mathbb{X}\lambda^2\mathbb{X}^{-1}, \tag{5}$$

where $\mathbb{X}$ is the matrix of eigenvectors, $\mathbb{X}^{-1}$ is the inverse of $\mathbb{X}$, and λ^2 is the diagonal matrix of eigenvalues. The solution to Eq. (3) subject to the boundary conditions (4) is then

$$\mathbb{C}(x) = \mathbb{X}\left\{\cosh(\lambda_i x) - \frac{\sinh(\lambda_i x)}{\tanh(\lambda_i l)}\right\}\mathbb{X}^{-1}\mathbb{C}_{(i)} + \mathbb{X}\left\{\frac{\sinh(\lambda_i x)}{\sinh(\lambda_i l)}\right\}\mathbb{X}^{-1}\mathbb{C}_{(j)}, \tag{6}$$

where the expressions within the braces are diagonal matrices, x is the axial coordinate in any particular capillary between nodes (i) and (j) of the network, and (i) is the origin with respect to the local value of x; i.e., each pore is treated separately.

The molar flux of the components into a pore from one of the adjacent sites (i) and (j) can then be expressed as a linear function of the two terminal node concentration vectors:

$$\mathbb{N}_{(i,j)} = -\Pi R^2_{(i,j)}\,\mathbb{D}\,(\nabla\mathbb{C}\,|_{x=0})_{(i,j)} \quad \text{and}$$

$$\mathbb{N}_{(i,j)} = \Pi R^2_{(i,j)}\,\mathbb{D}\mathbb{X}\{\lambda_i/\tanh(\lambda_i l)\}\mathbb{X}^{-1}\mathbb{C}_{(i)} + \Pi R^2_{(i,j)}\,\mathbb{D}\mathbb{X}\{-\lambda_i/\sinh(\lambda_i l)\}\mathbb{X}^{-1}\mathbb{C}_{(j)}. \tag{7}$$

The conservation of mass is imposed at each internal node by setting the algebraic sum of transformed fluxes to zero at these points (*11*). For the node (i) this can be expressed as

$$\mathbb{N}_{(i,i-N)} + \mathbb{N}_{(i,i-1)} + \mathbb{N}_{(i,i+1)} + \mathbb{N}_{(i,i+N)} = \mathbb{O}. \tag{8}$$

Equation (8) represents a set of three linear algebraic equations relating the concentration of the reagent (C_R) and the two product concentrations (C_A and C_B) at a particular node to the concentrations of the three species at the same and the surrounding nodes.

A material balance over the fluid phase giving the exchange with the pellet in the surface pores of the network is given by

$$\frac{d\mathbb{C}_m}{dX} = -\frac{\tau(1-\varepsilon_C)\,\varepsilon_P}{V_{PS}\,\varepsilon_C}\sum_{j=2}^{N+1}\mathbb{N}_{(1,j)}, \tag{9}$$

where X is the dimensionless axial position ($=X'/L$), τ is the reactor retention time ($=L/\langle v\rangle$), V_{PS} is the intraparticle pore volume, and ε_C and ε_P are the column and the particle porosity, respectively. At the entrance of the reactor

$$\mathbb{C}^T_m(X=0) = \{C_{m_R}(0), C_{m_A}(0), C_{m_B}(0)\} = \{1, 0, 0\}. \tag{10}$$

In order to obtain a complete description of the system, the internal site mass balances, Eq. (8), need to be joined to Eq. (9). This is done by assuming the fluid phase concentration ($\mathbb{C}_m$) for any pellet to be equal to the concentration ($\mathbb{C}_{(1)}$) at the pellet surface,

$$\mathbb{C}_m(X) = \mathbb{C}_{(1)}, \tag{11}$$

i.e., no pellet film transfer limitation.

The nodal mass balances take the matrix form

$$\mathbf{A}\,\mathbf{C}\,(X) = \mathbf{B}(X), \tag{12}$$

where $\mathbf{C}$ is the vector of nodal concentration vectors, $\mathbf{A}$ is a *conductance* matrix of matrices, and $\mathbf{B}$ represents the contribution from the mobile phase to the nodes in the neighbourhood of the inlet node of the network. Since the pellet has the same structure at each axial position, matrix $\mathbf{A}$ is spatially independent and can be inverted by standard routines for real sparse matrices so that

$$\mathbf{C}(X) = \mathbf{A}^{-1}\mathbf{B}(X). \tag{13}$$

The system of ordinary differential equations (9) is then numerically solved, e.g., by using a fourth-order Runge–Kutta method. At each step, the derivatives in Eq. (9) are evaluated from the solution of (13) together with the molar fluxes in the surface pores.

TABLE 1

Parameters Employed in the Simulations

Network dimension (N)	20×20
Particle length (l_P)	1.0
Capillary length (l)	$l_P/(N+1)$
Column voidage (ε_C)	0.5
Particle porosity (ε_P)	0.5
Radius factor (α)	0.1
Reactor retention time (τ)	1.0
Diffusivity matrix ($\mathbb{D}$)	

$$\mathbb{D}(R_1) = D_0 \begin{bmatrix} 1000 & 0 & 0 \\ 0 & 1 & 0 \\ 0 & 0 & 1000 \end{bmatrix}$$

$$\mathbb{D}(R_2) = D_0 \begin{bmatrix} 1000 & 0 & 0 \\ 0 & 1000 & 0 \\ 0 & 0 & 1000 \end{bmatrix}$$

Reaction rate constant matrix ($\mathbb{K}$)

$$\mathbb{K}(R_1) = \mathbb{O}$$

$$\mathbb{K}(R_2) = K_0 \begin{bmatrix} 2 & 0 & 0 \\ -1 & 1 & -2 \\ -1 & -1 & 2 \end{bmatrix}$$

5. RESULTS AND DISCUSSION

Average values of the reactant and product concentrations taken from five samples of a 20×20 network for a given Thiele modulus,

$$\phi = l_P \left(\frac{K_0}{D_0}\right)^{1/2}, \tag{14}$$

for a given value of the small radius frequency p1, have been used to calculate the conversion

$$\chi_R = 1 - C_{m_R}(1)/C_{m_R}(0), \tag{15}$$

and the selectivity of the product B,

$$\mathcal{S}_B = C_{m_B}(1)/[C_{m_A}(1) + C_{m_B}(1)], \tag{16}$$

at the exit of the reactor ($X = 1$).

The physicochemical and structural parameters used in the simulations are listed in Table 1. The diffusion of product A is severely *hindered* in the small radius pores, being only one thousandth of that in the large pores. This is a case where the A molecules are in the *configurational diffusion regime* (5).

Figure 3 shows how the conversion is influenced by the frequency of the smaller radius for different values of the Thiele modulus. When the Thiele modulus is small, the effectiveness is very high. The reaction predominates over the diffusion so the conversion is high and uninfluenced by the number of small pores. On the other hand, when ϕ is large (e.g., $\phi = 200$), the extent of reaction is severely reduced and essentially confined to the surface pores of the pellet. It progressively decreases as the frequency (number) of the smaller pores increases because reaction does not take place in some parts of the catalyst. At intermediate values of ϕ (e.g., $\phi = 20$) there is competition between diffu-

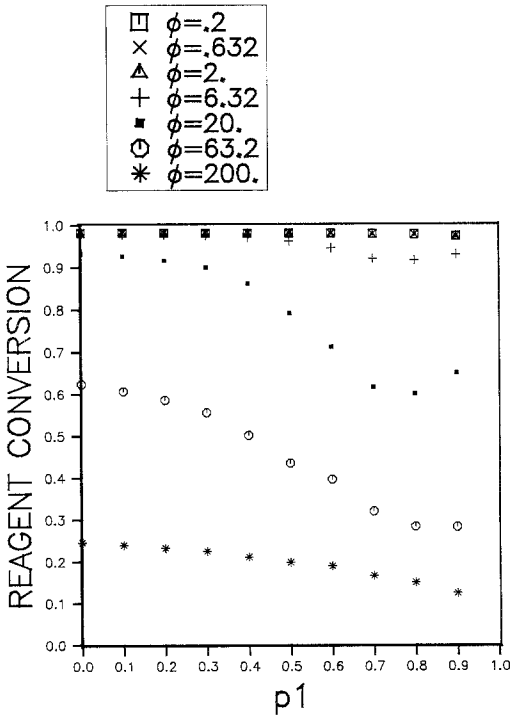

FIG. 3. Dependence of the reagent conversion (χ_R) on the frequency of the smaller pore (p1) for different Thiele modulus conditions.

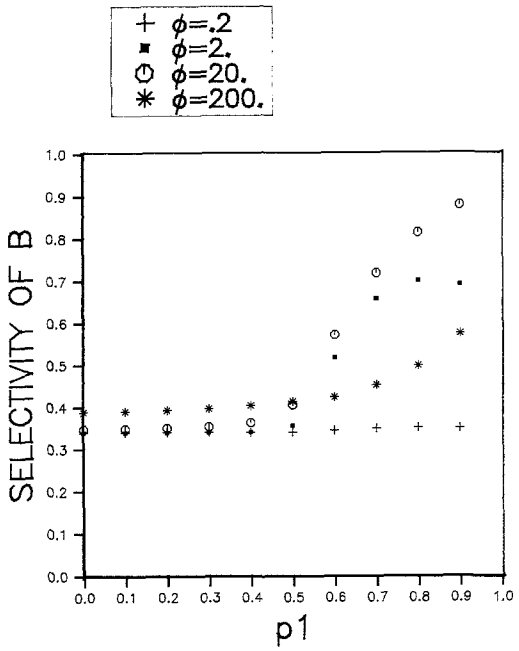

FIG. 4. Dependence of the selectivity of the product B ($\mathcal{S}_B$) on the frequency of the smaller pore (p1) for different Thiele modulus conditions.

sion and chemical reaction, and the extent of reaction is particularly sensitive to the structural detail of the pore volume. This can be seen in Fig. 3 where a minimum conversion occurs around a frequency p1 equal to 0.8. Another previous study (*13*) has shown that predicted tortuosity factors for randomly generated square networks are anomalously high for this value of p1. This can be interpreted directly in terms of the frequency (1 − p1) and spatial arrangement of the large pores which control the overall mass transfer in the pore structure.

Figure 4 shows how the selectivity of the product B is affected by the small radius frequency and the Thiele modulus. When $\phi = 0.2$ there is no diffusion resistance to mass transfer in the pores and the secondary reactions (A → B and B → A) are able to generate a product distribution which is very near to the equilibrium partition of 33.3% B and 66.6% A. When $\phi = 200$, there is a progressive increase in selectivity of B as p1 increases. This is a consequence of the so-called *bottleneck effect* caused by the large pores in the network being completely *shielded* by small ones. In this situation, the difference in the diffusion coefficients of products, arising from steric factors, combines with the reversible secondary reactions to increase the selectivity of B because of its large diffusion coefficient. The tortuosity of the catalyst pore structure obviously plays a significant role in modifying the B-selectivity pattern. As the Thiele modulus decreases, there is a gradual change in the shape of the B-selectivity curve. The monotonic behaviour observed when $\phi = 200$ changes to a curve exhibiting a maximum $\mathcal{S}_B$ value around p1 = 0.8 at $\phi = 2$. For this value of the Thiele modulus, there is an optimal number and spatial arrangement of bottleneck cavities in terms of B-selectivity which is intimately associated with the highly tortuous diffusion paths followed by the reactants and products.

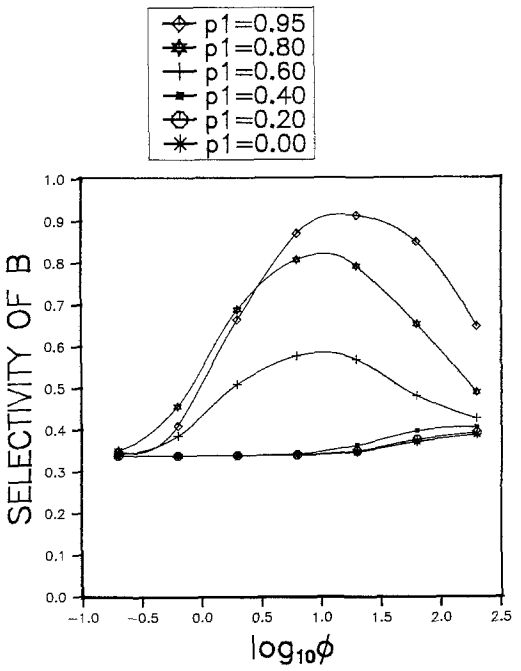

FIG. 5. Dependence of the selectivity of the product B ($\mathcal{S}_B$) on the Thiele modulus for different values of the frequency of the smaller pore (p1).

Referring to Figs. 3 and 4, it can be seen that high selectivities of product B always occur at p1 values of relatively low reagent conversions, which is consistent with the experimental results reported by Kaeding *et al.* (*1*) for the selective alkylation of toluene with methanol to produce *para*-xylene using modified ZSM-5 zeolites. As a feature of practical interest, it could suggest a strategy for recycling and recovering the reagent with respect to the yield of the desired product.

The overall effects of structure on performance depend on taking account of physicochemical and structural variables simultaneously, and any particular problem requires the complex interactions between them to be understood. Figure 5 shows that these variables must be balanced in a reactor design, especially if they are likely to change during operation, as when temperature might be changed (ϕ) to compensate for variations in the pore structure (e.g., due to coke deposition). The model is useful in giving some insight as to the way these changes could be made.

6. CONCLUSIONS

The influence of sterically hindered diffusion on catalytic reaction schemes has been examined with specific reference to pore structure using computer simulation of the transport processes. The model provides a description of those factors influencing shape selectivity which have particular relevance to zeolites and other highly structured supports. A basis is provided for relating shape selectivity to diffusional, kinetic factors as well as to the structure of the catalyst support. This provides useful insight as to those factors which can be expected to significantly improve yields of specific products in shape selective catalytic reactions, and is illustrated by reference to a means of improving the separation of isomers.

ACKNOWLEDGMENTS

One of us, J. S. Andrade, Jr., expresses his gratitude to the Brazilian agency CNPq for financial support.

REFERENCES

1. Kaeding, W. W., Chu, C., Young, L. B., Weinstein, B., and Butter, S. A., *J. Catal.* **67,** 159 (1981).
2. Kaeding, W. W., Chu, C., Young, L. B., and Butter, S. A., *J. Catal.* **69,** 392 (1981).
3. Young, L. B., Butter, S. A., and Kaeding, W. W., *J. Catal.* **76,** 418 (1982).
4. Wei, J., *J. Catal.* **76,** 433 (1982).
5. Weisz, P. B., *Pure Appl. Chem.* **52,** 2091 (1980).
6. Ruthven, D. M., *Can. J. Chem.* **52,** 3523 (1974).
7. Wakao, N., Nardse, Y., *Chem. Eng. Sci.* **29,** 1304 (1974).
8. Mo, W. T., and Wei, J., *Chem. Eng. Sci.* **41,** 703 (1986).
9. Mann, R., Sharrat, P. N., and Thompson, G., *Chem. Eng. Sci.* **41,** 711 (1986).
10. Sharrat, P. N., and Mann, R., *Chem. Eng. Sci.* **42,** 1565 (1987).
11. Mann, R., and Sharrat, P. N., *Chem. Eng. Sci.* **43,** 1875 (1988).
12. Topsøe, N. Y., Pedersen, K., and Derouane, E., *J. Catal.* **70,** 41 (1981).
13. Rajagopal, K., Andrade, J. S., Jr., and McGreavy, C., *Chem. Eng. Sci.,* submitted for publication.